

Article

Effect of Ultrafine Metakaolin on the Properties of Mortar and Concrete

Shengli Zhang ¹, Yuqi Zhou ², Jianwei Sun ^{3,*} and Fanghui Han ⁴¹ Beijing Urban Construction Engineering Co., Ltd., Beijing 100071, China; shenglizhang@mail.buce.cn² China Construction First Group Construction and Development Co., Ltd., Beijing 100102, China; zhouyuqi@chinaonebuild.com³ School of Civil Engineering, Qingdao University of Technology, Qingdao 266033, China⁴ School of Civil and Resource Engineering, University of Science and Technology Beijing, Beijing 100083, China; hanfanghui@ustb.edu.cn

* Correspondence: jianwei2019@mail.tsinghua.edu.cn

Abstract: This study investigated the influence of ultrafine metakaolin replacing cement as a cementitious material on the properties of concrete and mortar. Two substitution levels of ultrafine metakaolin (9% and 15% by mass) were chosen. The reference samples were plain cement concrete sample and silica fume concrete sample with the same metakaolin substitution rates and superplasticizer contents. The results indicate that simultaneously adding ultrafine metakaolin and a certain amount of polycarboxylate superplasticizer can effectively ensure the workability of concrete. Additionally, the effect of adding ultrafine metakaolin on the workability is better than that of adding silica fume. Adding ultrafine metakaolin or silica fume can effectively increase the compressive strength, splitting tensile strength, resistance to chloride ion penetration and freeze–thaw properties of concrete due to improved pore structure. The sulphate attack resistance of mortar can be improved more obviously by simultaneously adding ultrafine metakaolin and prolonging the initial moisture curing time.

Keywords: ultrafine metakaolin; silica fume; strength; durability

Citation: Zhang, S.; Zhou, Y.; Sun, J.; Han, F. Effect of Ultrafine Metakaolin on the Properties of Mortar and Concrete. *Crystals* **2021**, *11*, 665. <https://doi.org/10.3390/cryst11060665>

Academic Editors: Yifeng Ling, Chuanqing Fu, Peng Zhang and Peter Taylor

Received: 21 May 2021
Accepted: 8 June 2021
Published: 10 June 2021

Publisher's Note: MDPI stays neutral with regard to jurisdictional claims in published maps and institutional affiliations.



Copyright: © 2021 by the authors. Licensee MDPI, Basel, Switzerland. This article is an open access article distributed under the terms and conditions of the Creative Commons Attribution (CC BY) license (<https://creativecommons.org/licenses/by/4.0/>).

1. Introduction

Concrete made with Portland cement has been available for nearly two hundred years. In the past two centuries, with the development of science and technology, the composition and performance of Portland cement have undergone great changes, and construction technology using concrete has also undergone earth-shaking changes [1,2]. The two changes above have led to complete changes in the composition, preparation methods and performance of modern concrete. Mineral admixtures such as supplementary cementitious materials are an indispensable part of modern concrete [3,4]. The use of high-activity admixtures such as slag and low-activity or inert admixtures such as limestone powder effectively reduces energy and resource consumption by decreasing the amount of cement used in the concrete production process and ensures the green and sustainable development of the concrete industry [3,4]. More importantly, the use of admixtures reduces the dependence of modern concrete strength on cement strength, improves the rheological properties of the mixture, and increases the durability of concrete structures.

At present, the mineral admixtures used in the concrete preparation process worldwide are mainly fly ash, slag, and limestone powder [5–8]. However, with the development of the concrete industry, the stock of high-quality admixtures has decreased, leading to gradually rising prices. Therefore, the available high-quality and economical mineral admixtures will become increasingly scarce and unable to meet the needs of the national construction market. On the premise that the annual production of admixtures cannot be changed, the main technical means to offset the scarcity of high-quality admixtures

is to increase their reactivity to reduce the dosage. Mechanical grinding is the most direct method used to improve the reactivity of powders. Ultrafine grinding involves the application of strong mechanical forces that distort the crystal structure of the mineral, rapidly resulting in lattice dislocations, defects, and recrystallization, which improves the reaction activity [9–12]. On the other hand, ultrafine grinding increases the specific surface area of the admixture, thereby enhancing micro aggregation and nucleation effects in the cement matrix [13–15]. In addition, ultra-high-performance concrete (UHPC) has attracted increasing attention due to it meeting the requirements for special concrete structures such as super high-rise buildings and long-span bridges [16–18]. Ultra-high-activity mineral admixtures, such as ultrafine powders, are indispensable for the preparation of UHPC [19–21]. Therefore, it is necessary to study the action mechanism and application effects of ultrafine admixtures in concrete, whether from the perspective of improving the overall quality of admixtures, solving the problem of the scarcity of high-quality admixtures, or meeting the needs of special engineering and ensuring the supply of UHPC.

Metakaolin is an amorphous aluminum silicate formed by the calcination of kaolin clay at temperatures ranging from 500 °C to 800 °C [22,23]. In the process of heating, most octahedral alumina is converted into more active tetra-coordinated and penta-coordinated units [24,25]. When the crystal structure is completely or partially broken, or the bonds between the kaolinite layers are broken, kaolin undergoes a phase change and finally forms metakaolin with poor crystallinity [25,26]. As its molecular arrangement is irregular, metakaolin is in a metastable thermodynamic state and has gelling properties under appropriate excitation [23–26]. Metakaolin has high pozzolanic activity, which means that it can react with $\text{Ca}(\text{OH})_2$ and produce C-S-H gel and alumina-containing phases, including C_4AH_{13} , C_2ASH_8 , and C_3AH_6 , at ambient temperature [23]. Therefore, metakaolin is mainly used as a mineral admixture in cement and concrete. Compared to silica fume and fly ash, metakaolin has a very high reactivity level [23]. Previous studies have shown that metakaolin can increase the mechanical strength of concrete to varying degrees, depending mainly on the replacement rate of metakaolin, the water/binder ratio, and the age at testing [22,23,27]. Remarkably, metakaolin has a positive effect on reducing drying shrinkage and improving durability [22,23,27–30].

In current practical engineering applications, 99.9% of metakaolin particles are less than 16 μm [23]. The mean particle size is generally 3 μm , which is significantly smaller than that of cement particles but not as fine as silica fume [23]. Ultrafine metakaolin with a specific surface area greater than 20,000 m^2/kg can be obtained by grinding. The pozzolanic activity of metakaolin is related to the particle size. Theoretically, it is practical to grind metakaolin so that it can play a greater role in concrete. In this paper, ultrafine metakaolin obtained by grinding was used as a supplementary cementitious material in concrete and mortar. The macroscopic properties, including the mechanical strength and durability of concrete and mortar, were investigated. Plain cement concrete and silica fume concrete were employed as reference samples.

2. Materials and Methods

2.1. Raw Materials

In this paper, Portland cement with a strength grade of 42.5 from Beijing Jinyu Group Co., Ltd. in China was used as the cementitious material. Ultrafine metakaolin and silica fume with similar specific surface areas were used as mineral admixtures. The chemical compositions of the raw materials are presented in Table 1. The total content of SiO_2 and Al_2O_3 in ultrafine metakaolin is more than 99%. The particle size distribution of ultrafine metakaolin is shown in Figure 1a. The X-ray diffraction (XRD) patterns of ultrafine metakaolin are presented in Figure 1b. Figure 1b shows that the amorphous phase is the main constituent, and SiO_2 crystals are the main crystalline mineral phase in ultrafine metakaolin. The microstructure of ultrafine metakaolin is shown in Figure 1c. Ultrafine metakaolin is broken into small angular particles. Fine aggregates of mortar and concrete were ISO standard sand and river sand with a fineness modulus of 2.9, respectively.

Crushed limestone with a continuous size gradation from 4.75 mm to 20 mm was used as coarse aggregate. A polycarboxylate superplasticizer with a water reduction rate of 20% was used to adjust the flowability of fresh mortar and concrete.

Table 1. Main chemical compositions of raw materials/%.

	CaO	SiO ₂	Al ₂ O ₃	Fe ₂ O ₃	MgO	SO ₃	Na ₂ O _{eq} *	LOI
Cement	54.86	21.10	6.33	4.22	2.60	2.66	0.53	2.03
Ultrafine Metakaolin	0.13	52.72	46.29	0.28	0.15	0.08	0.12	0.64
Silica Fume	-	94.67	-	-	-	-	0.06	2.51

* Na₂O_{eq} = Na₂O + 0.658K₂O; LOI: loss on ignition.

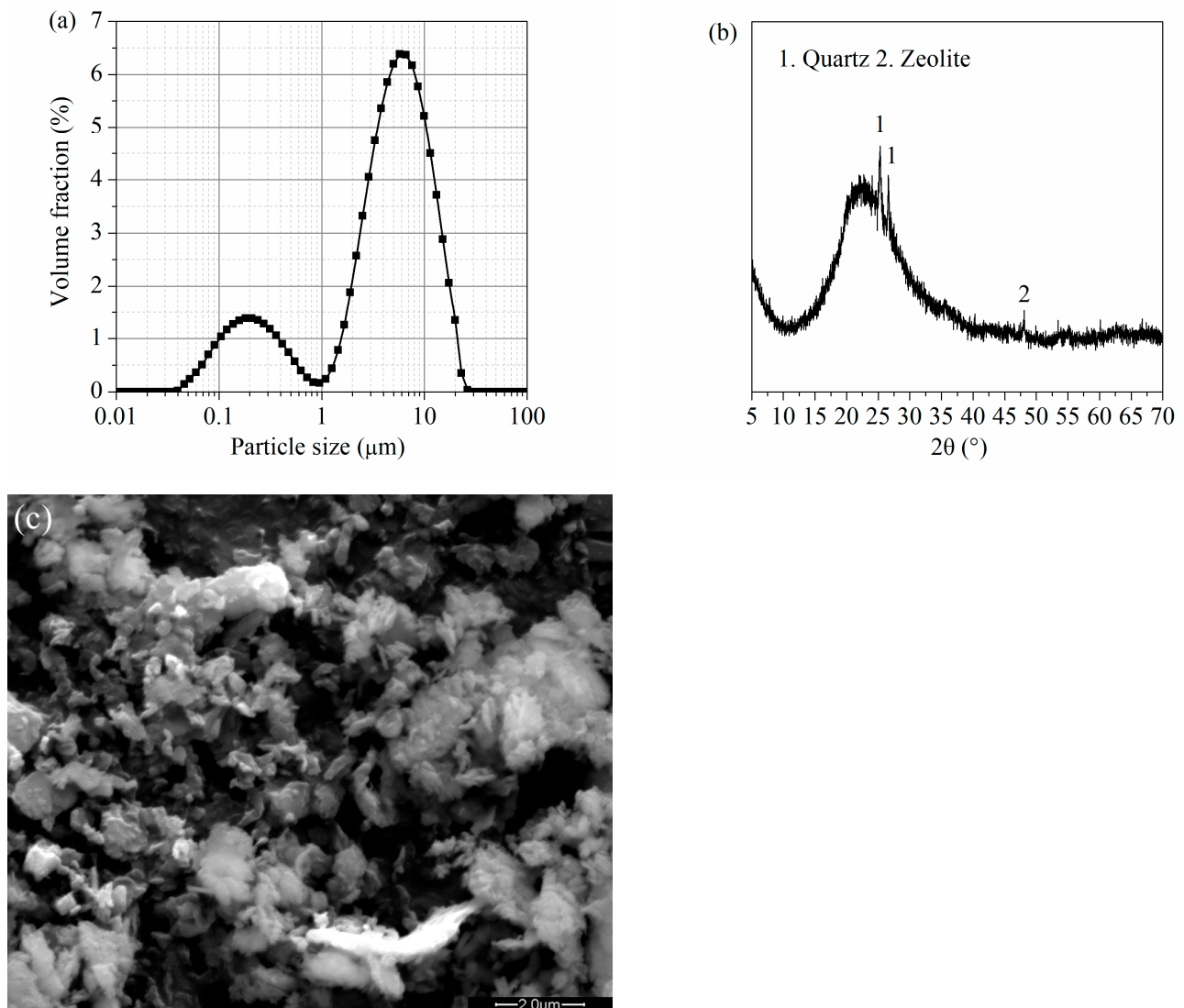


Figure 1. Characteristics of ultrafine metakaolin used in this study: (a) particle size distribution; (b) XRD analysis; (c) micromorphology.

2.2. Mix Proportions

Table 2 shows the mix proportions of concrete. The total amount of binder was 400 kg/m³. A water/binder ratio of 0.4 and a sand ratio of 0.44 were selected. Two substitution rates of ultrafine metakaolin (9% and 15% by mass) were used, corresponding to sample M1 and sample M2. The plain cement concrete sample (sample C), concrete sample containing 9% silica fume (sample S1) and concrete sample containing 15% silica

fume (sample S2) were regarded as the reference samples. The superplasticizer dosages by mass percent of the total cementitious materials in samples C, M1 and M2 were 0.8%, 0.85% and 0.95%, respectively. The fresh concrete was poured into different sizes of molds, including 100 mm × 100 mm × 100 mm and 100 mm × 100 mm × 400 mm. Only three mix proportions (samples C, M1 and M2) were used for the mortar test. The water/binder ratio was the same as concrete (0.4), and the sand/binder ratio was 3.0. Fresh mortar was poured into steel molds with dimensions of 40 mm × 40 mm × 160 mm for sulphate attack test. After 24 h, all samples were unmolded and cured under scheduled regimes.

Table 2. Mix proportions of concretes/kg·m⁻³.

Sample	Cement	Ultrafine Metakaolin	Silica Fume	Fine Aggregate	Coarse Aggregate	Water	Superplasticizer
C	400	0	0	854	1086	160	3.2
M1	364	36	0	854	1086	160	3.4
S1	364	0	36	854	1086	160	3.4
M2	340	60	0	854	1086	160	3.8
S2	340	0	60	854	1086	160	3.8

2.3. Curing Conditions and Test Methods

In the fresh state, the workability of fresh concrete was determined according to Chinese National Standard GB/T 50080-2016. The fresh concrete was poured into the slump bucket (upper 100 mm, lower 200 mm, and height 300 mm). After each pouring, a tamper bar was used to hammer it evenly 25 times. After tamping, the bucket was pulled up, and the concrete collapsed due to its own weight. The height value after the slump was recorded. The slump value and loss ratio were calculated by the height difference between peak height and slump height. In this study, different methods were used to cure concrete and mortar. Concrete was cured under standard curing conditions at a constant temperature (20 ± 2 °C) and relative humidity ($95 \pm 1\%$). The compressive strength of concrete after 1 d, 3 d, 7 d, 28 d and 90 d and the splitting tensile strength after 28 d and 90 d were measured according to China National Standards GB/T 50081-2011. Tests of compressive strength and splitting tensile strength were performed after casting at a certain age by using three specimens for each test. The chloride ion penetrability resistance and freeze–thaw resistance of concrete were determined by the American Society of Testing Materials Standard ASTM C1202 and Chinese National Standard GB/T 50082-2009, respectively. For the chloride ion penetrability resistance test, the cube specimen of 100 mm × 100 mm × 100 mm was used to cut one specimen of 50 mm × 100 mm × 100 from the middle. The charge passed in 6 h was used to evaluate the chloride ion penetrability resistance. Three test blocks were tested for each group of specimens. For the freeze–thaw resistance test, 100 mm × 100 mm × 100 mm cube blocks were used. The mass change and dynamic elasticity modulus were tested after 300 cycles. The average value for six specimens was obtained to ensure the accuracy of the test. For the connected porosity test, the cut specimen of 50 mm × 100 mm × 100 mm was used. The connected porosity was measured by the vacuum saturation–drying method. The connected porosity P was determined using the Equation (1):

$$P = (m_1 - m_2)/m_1 \times 100\%, \quad (1)$$

where m_1 is the mass of concrete that was completely saturated with water by the vacuum saturation method for 3 d and m_2 represents the mass of concrete that was dried at 40 °C for 14 d.

Two curing conditions for mortar were used: 3 d and 7 d initial moist curing. After initial moist curing, all mortars were placed in a natural environment. The compressive strength was tested after 28 d, and then the mortar was semi-immersed in a solution containing 10% sodium sulphate (by mass) for 28 d, 56 d and 90 d. The concentration of the sodium sulphate solution was maintained by periodically replacing the solution. Meanwhile, the reference specimens cured in water for the same lengths of time were tested for compressive strength and flexural strength. Therefore, the sulphate attack resistance was evaluated by the relative compressive strength and flexural strength loss for the same curing time.

3. Results and Discussion

3.1. Workability

Table 3 presents the values of slump and slump loss for all mixtures with different dosages of ultrafine metakaolin. No segregation or bleeding was observed during mixture experiments. Obviously, the workability of fresh concrete and replacement rate of ultrafine metakaolin are nonlinearly related in Table 3. Compared to plain cement concrete, adding 9% ultrafine metakaolin decreases workability, while adding 15% ultrafine metakaolin has little influence on workability. The addition of 9% ultrafine metakaolin results in a smaller average particle size and larger specific surface area of the composite binder, which leads to the availability of less free water in the concrete matrix. Therefore, sample M1 has poorer workability. However, sample M2 has the highest content of superplasticizer compared to sample C, which seriously weakens the water absorption effect of ultrafine metakaolin particles. Compared to silica fume concrete with the same replacement rate and superplasticizer content, ultrafine metakaolin concrete has a higher slump value. This indicates that the compatibility of the superplasticizer and ultrafine metakaolin concrete is better. After 0.5 h, the slump loss values show the same change tendency as the slump. However, the slump loss ratio is significantly changed. Compared to plain cement concrete, adding 9% ultrafine mineral admixtures and 6.25% polycarboxylate superplasticizer has little influence on the slump loss ratio. The addition of 15% ultrafine mineral admixtures and 18.75% polycarboxylate superplasticizer obviously decreases the slump loss ratio. Adding ultrafine metakaolin has a more effective impact.

Table 3. Slump and slump loss of fresh concretes.

	C	M1	S1	M2	S2
0 h (mm)	235	224	213	233	221
0.5 h (mm)	180	172	162	186	172
Loss ratio (%)	23.40	23.21	23.94	20.17	22.17

3.2. Mechanical Strength

The compressive strength and splitting tensile strength of all concrete are shown in Figure 2. Overall, adding mineral admixtures increases the compressive strength of concretes at all ages, as shown in Figure 2a. It is more obvious at the later ages. However, different admixture dosages have various effects on ultrafine metakaolin concrete. The compressive strength of sample M1 is slightly higher than that of sample M2 at 1 d, and it is obviously higher than that of sample M2 at 3 d and 7 d. At 1 d, the early compressive strengths of all concretes are approximately 15 MPa. At 3 d, the compressive strength of plain cement concrete is 30 MPa, while the maximum strength is nearly 40 MPa (sample M1). At 7 d, the compressive strengths of all concretes increase by approximately 10 MPa. However, the opposite trend occurs at 28 d and 90 d. At 28 d, the compressive strengths of sample C and sample M1 increase by approximately 10 MPa, but the compressive strength of sample M2 reaches 62 MPa, increasing by 17 MPa. Therefore, adding 15% ultrafine metakaolin can increase the strength of concrete to meet the strength requirements of C60. The compressive strength of the composite concrete increases slowly from 28 d to 90 d. Thus, sample M2 has the highest compressive strength at late ages. Compared

to plain cement concrete, adding 15% ultrafine metakaolin increases the compressive strength at 28 d and 90 d by 24% and 20%, respectively. There is not much difference in the compressive strengths of ultrafine metakaolin concrete and silica fume concrete with the same replacement rate and superplasticizer content at all ages. Remarkably, the 7 d compressive strengths of all concretes reached nearly 72–83% of the 28-d strength, which suggests that a high superplasticizer content has no obvious negative effect on the early strength of concrete.

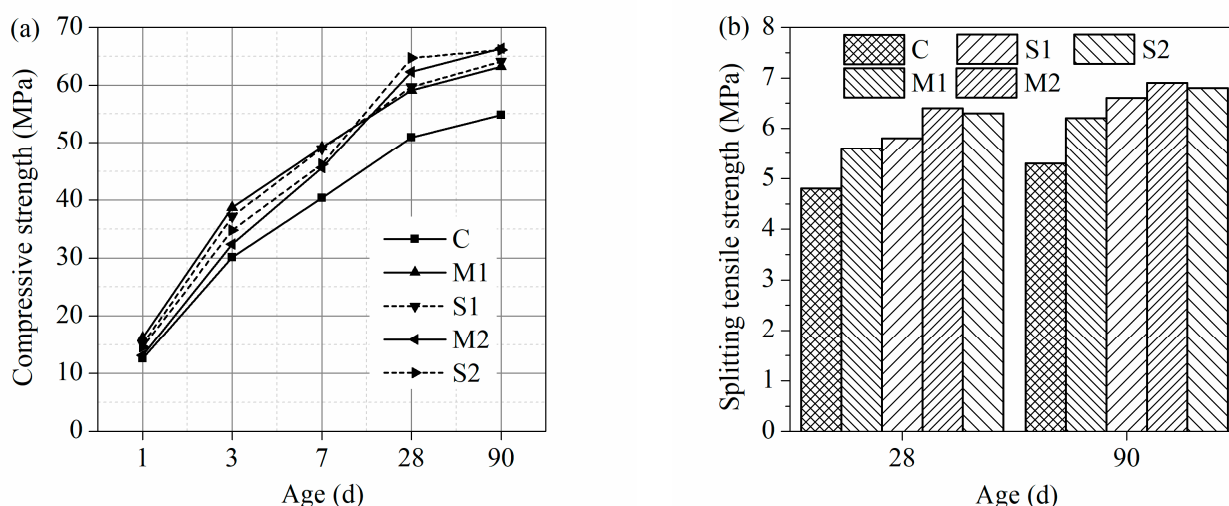


Figure 2. Mechanical strength of concrete: (a) compressive strength; (b) splitting tensile strength.

Figure 2b shows the same influence of ultrafine mineral admixtures on the splitting tensile strength and compressive strength. The results show that the splitting tensile strength of concrete increases as the ultrafine admixture content increases. There is little difference in the splitting tensile strength of ultrafine metakaolin concrete and silica fume concrete with the same replacement rate and superplasticizer content at 28 d and 90 d. Adding 9% ultrafine metakaolin increases the splitting tensile strength by approximately 17% at 28 d and 90 d. Adding 15% ultrafine metakaolin increases the splitting tensile strength at 28 d and 90 d by approximately 33% and 30%, respectively. The maximum splitting tensile strength is close to 7 MPa at 90 d (samples M2 and S2).

3.3. Connected Porosity

The connected porosity of concrete is an index used to measure the transport capacity of water and solution erosion, which is closely related to permeability. The connected porosities of all concretes at 28 d are shown in Figure 3. Remarkably, the 28-d connected porosity values of all concretes are in the 11–14% range. As shown in Figure 3, the connected porosity of concrete obviously decreases with increasing ultrafine metakaolin content. The connected porosity of silica fume concrete is relatively lower than that of ultrafine metakaolin concrete at the same replacement rate and superplasticizer content. This indicates that the addition of ultrafine mineral admixtures refines the pore structure of concrete and makes the matrix denser, which improves the durability of concrete. This result is consistent with the findings of Erhan et al. [22], who found that ultrafine metakaolin substantially enhanced the pore structure of concrete and reduced the presence of harmful large pores, especially at a high replacement level. The beneficial effect of adding silica fume is slightly better than that of adding ultrafine metakaolin.

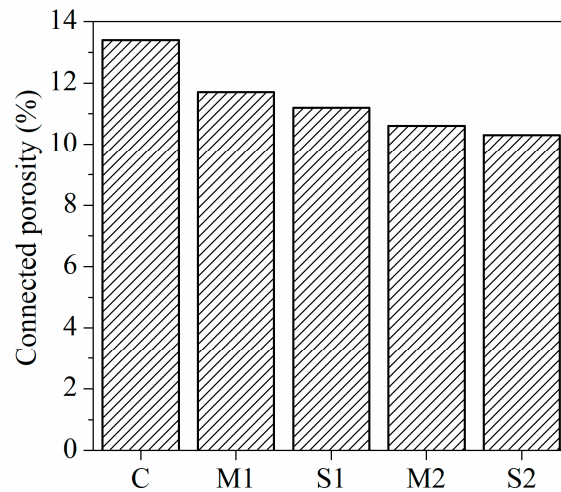


Figure 3. Connected porosity of concrete.

3.4. Chloride Ion Penetrability of Concrete

According to ASTM C1202, the penetrability grades of concrete at 28 d and 90 d are shown in Figure 4. Apparently, Figure 4 shows that the penetrability grades of samples C, M1 and M2 at 28 d are “moderate”, “low” and “very low”, respectively. At 90 d, although the charge passed by all concretes decreases due to lower connected porosity, there is no change in penetrability levels. Meanwhile, the penetrability grades of ultrafine metakaolin concrete and silica fume concrete with the same replacement rate show little difference at 28 d and 90 d for the same superplasticizer content. This result is attributed to similar pore structures. Therefore, adding ultrafine mineral admixtures can improve the resistance to chloride ion penetration of concretes at 28 d and 90 d. Ultrafine metakaolin has the same effect as silica fume.

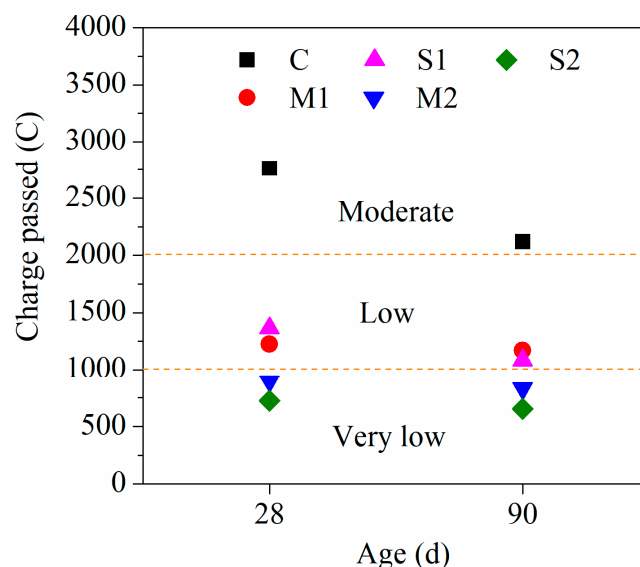


Figure 4. Chloride ion penetrability of concrete.

3.5. Freeze–Thaw Resistance

Freeze–thaw damage is the main factor affecting the instability of concrete structures in cold areas, which seriously threatens the safety and service life of concrete structures. The relative dynamic elasticity modulus and mass loss of all concretes after 300 freeze–thaw cycles are presented in Figure 5a,b, respectively. Figure 5a shows that the relative dynamic

elasticity moduli of samples M1–S2 are all 81–86% after 300 cycles; therefore, sample M2 has the best freeze–thaw resistance, and its relative dynamic elasticity modulus is 85.5%. However, the relative dynamic elasticity modulus of plain cement concrete is only 62.8%, which is much less than those of composite concretes. Figure 5b shows that the mass loss of plain cement concrete exceeds 5%. However, the mass loss of samples M1–S2 is very small, less than 4% after 300 cycles in Figure 5b. Therefore, ultrafine metakaolin concrete and silica fume concrete can meet the frost resistance requirements in cold areas; they have the lowest frost resistance grade of F300. With increasing ultrafine metakaolin or silica fume content, the relative dynamic elasticity modulus of concrete tends to increase, and the mass loss decreases obviously. Meanwhile, it can hardly observe surface denudation of samples M1, S1, M2 and S2, and the surface damage layers of these samples above are very thin. Thus, composite concrete has excellent apparent performance. Therefore, adding ultrafine metakaolin or silica fume has a positive influence on the freeze–thaw resistance of concrete.

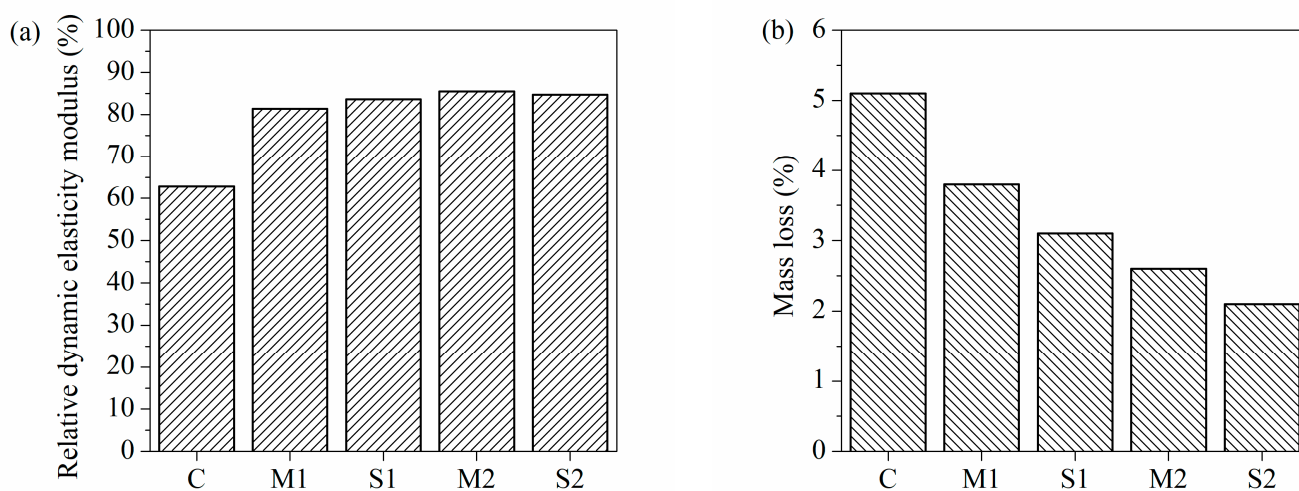


Figure 5. Results of fast freeze–thaw cycle tests of concretes after 300 cycles: (a) relative dynamic elasticity modulus; (b) mass loss.

3.6. Sulphate Attack

Figure 6 shows the influence of different initial moisture curing times on the 28-d compressive strength. The 28-d compressive strengths of samples C, M1 and M2 for 3-d initial moisture curing are 55.3 MPa, 59.1 MPa and 67.9 MPa, respectively. Compared to sample C, the growth rates of samples M1 and M2 are 6.9% and 22.8%, respectively. The 28-d compressive strengths of samples C, M1 and M2 for 7-d initial moisture curing are 57.4 MPa, 64.7 MPa and 70.8 MPa, respectively. Adding 9% and 15% ultrafine metakaolin increases the 28-d compressive strength by 12.7% and 23.3%, respectively. The strength growth rate of the 28-d compressive strength significantly increases with increasing ultrafine metakaolin content. The growth rate for 7-d initial moisture curing is higher than the growth rate for 3-d initial moisture curing. Meanwhile, compared to that for 3-d initial moisture curing, the 28-d compressive strength of mortar for 7-d initial moisture curing increases. The growth rates of samples C, M1 and M2 are 3.8%, 9.5% and 4.3%, respectively. The growth rates of samples M1 and M2 are higher than that of sample C. Therefore, prolonging the initial moisture curing time is more favorable for ultrafine metakaolin concrete than plain cement concrete.

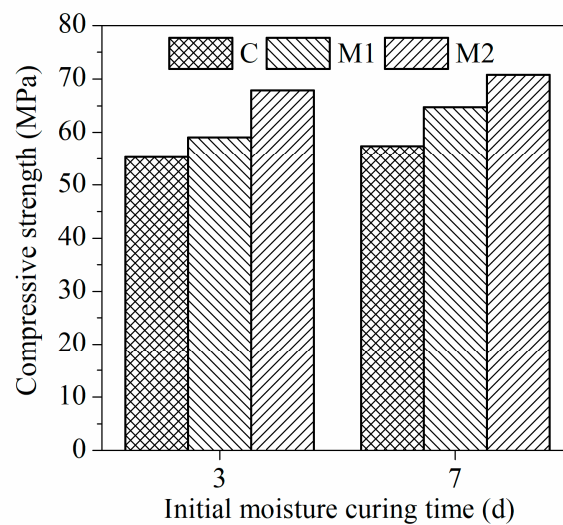


Figure 6. The 28-d compressive strength with different initial moisture curing time.

The visual appearance of samples C, M1 and M2 exposed to sulphate attack for different ages is shown in Figure 7a–c, respectively. The numbers marked in Figure 7 refer to the initial moisture curing time. Many salt crystals precipitate from the upper parts of the mortars and tend to increase with prolonged semi-immersion time. In the process of semi-immersion, no obvious cracks appear on the surfaces of all mortars. The relative compressive strengths of the mortars after different semi-immersion times are shown in Figure 8a. When the mortars were initially moisture cured for 3 d, the relative compressive strength of all mortars after 28 d of semi-immersion are less than 100%. However, the relative compressive strengths for certain mortars after 56 d and 90 d of semi-immersion are more than 100%, especially for plain cement mortar. When the mortars are initially moisture cured for 7 d, the relative compressive strengths of almost all mortars after semi-immersion are less than 100%. Therefore, from the results for the relative compressive strengths, prolonging the initial moisture curing time has an adverse effect on the sulphate attack resistance. This is unreasonable. Previous studies have shown that prolongation of the initial moisture curing time is beneficial to cement hydration and pore structure development, and sulphate attack resistance should not decrease with prolongation of the initial moisture curing time [23,27]. Therefore, the compressive strength cannot be used as an index to evaluate sulphate attack resistance of rectangular mortars in semi-immersion tests. The flexural strength losses of mortars after different semi-immersion times are shown in Figure 8b. Apparently, the flexural strength losses of mortars decrease with increasing ultrafine metakaolin at any semi-immersion age. When the semi-immersion time is the same, prolonging the initial moisture curing time has little impact on the flexural strength loss of samples C and M1. However, compared to the flexural strength loss for 3-d initial moisture curing, the flexural strength loss of sample M2 for 7-d initial moisture curing is relatively low. The addition of ultrafine metakaolin significantly improves the sulphate attack resistance of mortar, and the sulphate attack resistance also significantly improves with increasing ultrafine metakaolin. Therefore, in the semi-immersion test, it is reasonable to evaluate the sulphate attack resistance of mortar by flexural strength loss.

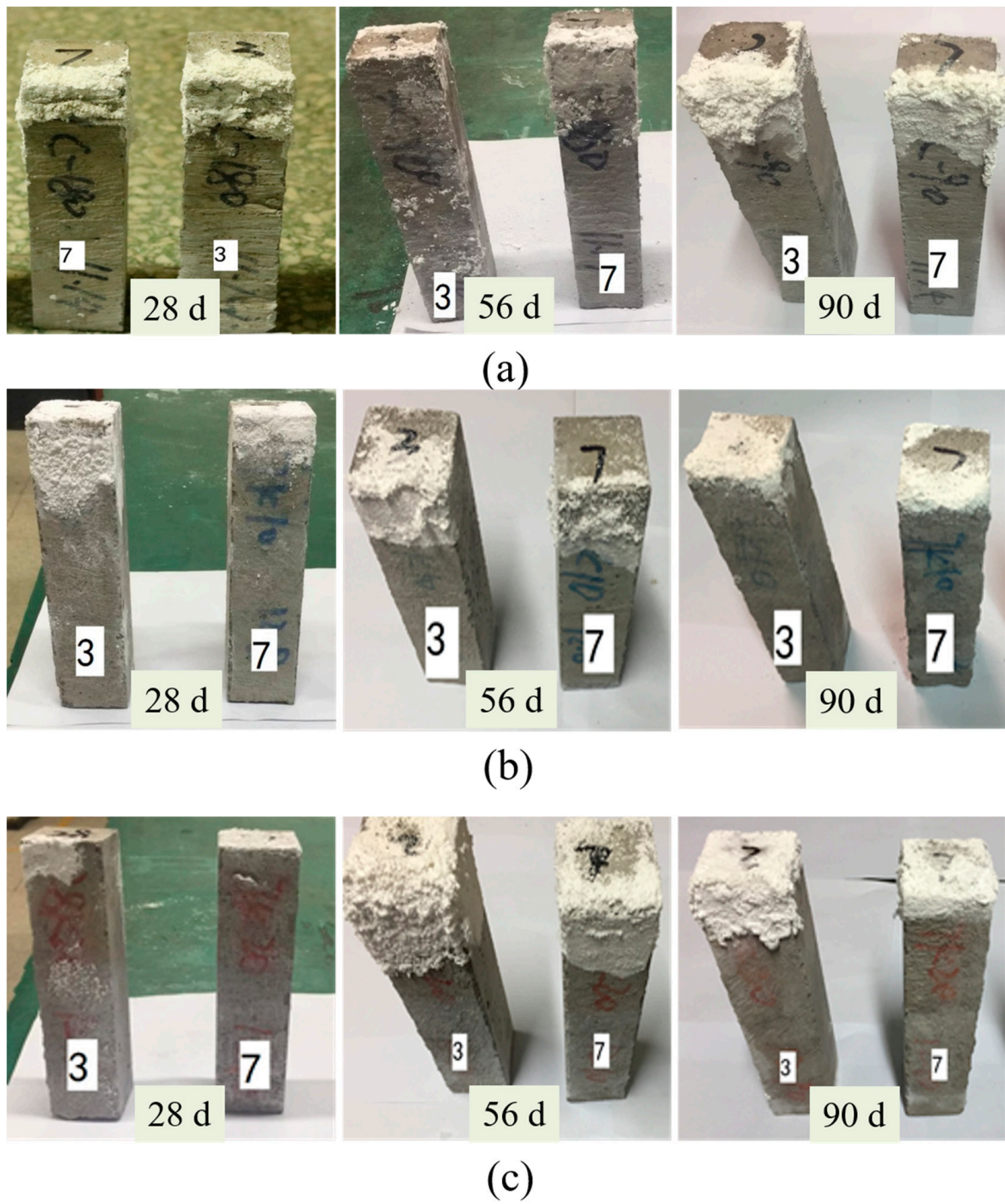


Figure 7. Visual appearance of mortar exposed to sulphate attack: (a) C; (b) M1; (c) M2.

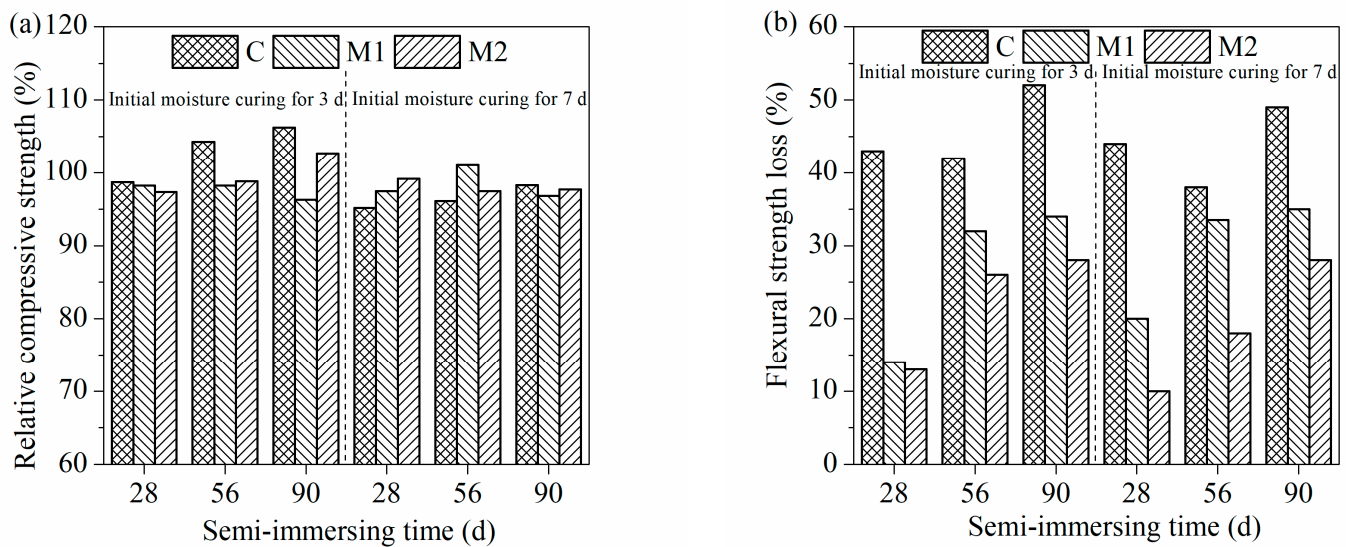


Figure 8. Results of sulphate attack: (a) relative compressive strength; (b) flexural strength loss.

4. Conclusions

- (1) Simultaneously adding ultrafine metakaolin and a certain amount of polycarboxylate superplasticizer can effectively ensure the workability of concrete. The effect of adding ultrafine metakaolin is better than that of adding silica fume in the same case.
- (2) The compressive strength and splitting tensile strength increase as the ultrafine admixture content increases. Adding 15% ultrafine metakaolin increases the compressive strength and splitting tensile strength at 28 d by approximately 24% and 33%, respectively. The effect of mixing the same amounts of ultrafine metakaolin and silica fume on the mechanical strength is not significant.
- (3) Adding ultrafine metakaolin obviously reduces the connected porosity of concrete, which effectively improves its resistance to chloride ion penetration and freeze–thaw cycles. Silica fume has the same effect as ultrafine metakaolin.
- (4) Prolonging the initial moisture curing time is more favorable for ultrafine metakaolin concrete than plain cement concrete in terms of compressive strength. Simultaneously adding ultrafine metakaolin and prolonging the initial moisture curing time can significantly improve the sulphate attack resistance of mortar.

Author Contributions: Conceptualization, S.Z.; methodology, Y.Z. and F.H.; software, S.Z. and Y.Z.; validation, J.S. and Y.Z.; writing—original draft preparation, J.S.; writing—review and editing, J.S. and F.H. All authors have read and agreed to the published version of the manuscript.

Funding: This research was funded by the National Natural Science Foundation of China (No. 51908033) and Beijing Natural Science Foundation (No. 8204067).

Institutional Review Board Statement: Not applicable.

Informed Consent Statement: Not applicable.

Data Availability Statement: Data are contained within the article.

Conflicts of Interest: The authors declare no conflict of interest.

References

1. Abedalqader, A.; Shatarat, N.; Ashteyat, A.; Katkhuda, H. Influence of temperature on mechanical properties of recycled asphalt pavement aggregate and recycled coarse aggregate concrete. *Constr. Build. Mater.* **2021**, *269*, 121285. [[CrossRef](#)]
2. Mei, S.; Wang, Y. Viscoelasticity: A new perspective on correlation between concrete creep and damping. *Constr. Build. Mater.* **2020**, *265*, 120557. [[CrossRef](#)]
3. Wang, D.; Wang, Q.; Huang, Z. Reuse of copper slag as a supplementary cementitious material: Reactivity and safety. *Resour. Conserv. Recycl.* **2020**, *162*, 105037. [[CrossRef](#)]

4. Wang, D.; Wang, Q.; Huang, Z. New insights into the early reaction of NaOH-activated slag in the presence of CaSO₄. *Compos. Part B Eng.* **2020**, *198*, 108207. [[CrossRef](#)]
5. Sun, J.; Chen, Z. Influences of limestone powder on the resistance of concretes to the chloride ion penetration and sulfate attack. *Powder Technol.* **2018**, *338*, 725–733. [[CrossRef](#)]
6. Sun, J.; Zhang, Z.; Hou, G. Utilization of fly ash microsphere powder as a mineral admixture of cement: Effects on early hydration and microstructure at different curing temperatures. *Powder Technol.* **2020**, *375*, 262–270. [[CrossRef](#)]
7. Wang, Q.; Feng, J.J.; Yan, P.Y. An explanation for the negative effect of elevated temperature at early ages on the late-age strength of concrete. *J. Mater. Sci.* **2011**, *46*, 7279–7288. [[CrossRef](#)]
8. Wang, Q.; Wang, D.; Chen, H. The role of fly ash microsphere in the microstructure and macroscopic properties of high-strength concrete. *Cem. Concr. Compos.* **2017**, *83*, 125–137. [[CrossRef](#)]
9. Yao, G.; Liu, Q.; Wang, J.; Wu, P.; Lyu, X. Effect of mechanical grinding on pozzolanic activity and hydration properties of siliceous gold ore tailings. *J. Clean. Prod.* **2019**, *217*, 12–21. [[CrossRef](#)]
10. Yao, G.; Cui, T.; Zhang, J.; Wang, J.; Lyu, X. Effects of mechanical grinding on pozzolanic activity and hydration properties of quartz. *Adv. Powder Technol.* **2020**, *31*, 4500–4509. [[CrossRef](#)]
11. Ting, L.; Qiang, W.; Shiyu, Z. Effects of ultra-fine ground granulated blast-furnace slag on initial setting time, fluidity and rheological properties of cement pastes. *Powder Technol.* **2019**, *345*, 54–63. [[CrossRef](#)]
12. Zhao, Y.; Gao, J.; Liu, C.; Chen, X.; Xu, Z. The particle-size effect of waste clay brick powder on its pozzolanic activity and properties of blended cement. *J. Clean. Prod.* **2020**, *242*, 118521. [[CrossRef](#)]
13. Irassar, E.F.; Bonavetti, V.L.; Castellano, C.C.; Trezza, M.A.; Rahhal, V.F.; Cordoba, G.; Lemma, R. Calcined illite-chlorite shale as supplementary cementing material: Thermal treatment, grinding, color and pozzolanic activity. *Appl. Clay Sci.* **2019**, *179*, 105143. [[CrossRef](#)]
14. Li, D.; Sun, R.; Wang, D.; Ren, C.; Fang, K. Study on the pozzolanic activity of ultrafine circulating fluidized-bed fly ash prepared by jet mill. *Fuel* **2021**, *291*, 120220. [[CrossRef](#)]
15. Yao, G.; Wang, Z.; Yao, J.; Cong, X.; Anning, C.; Lyu, X. Pozzolanic activity and hydration properties of feldspar after mechanical activation. *Powder Technol.* **2021**, *383*, 167–174. [[CrossRef](#)]
16. Ahmed, T.; Elchalakani, M.; Karrech, A.; Mohamed Ali, M.S.; Guo, L. Development of ECO-UHPC with very-low-C₃A cement and ground granulated blast-furnace slag. *Constr. Build. Mater.* **2021**, *284*, 122787. [[CrossRef](#)]
17. Herald Lessly, S.; Lakshmana Kumar, S.; Raj Jawahar, R.; Prabhu, L. Durability properties of modified ultra-high performance concrete with varying cement content and curing regime. *Mater. Today Proc.* **2020**. [[CrossRef](#)]
18. Ding, M.; Yu, R.; Feng, Y.; Wang, S.; Zhou, F.; Shui, Z.; Gao, X.; He, Y.; Chen, L. Possibility and advantages of producing an ultra-high performance concrete (UHPC) with ultra-low cement content. *Constr. Build. Mater.* **2021**, *273*, 122023. [[CrossRef](#)]
19. Lv, L.S.; Wang, J.Y.; Xiao, R.C.; Fang, M.S.; Tan, Y. Chloride ion transport properties in microcracked ultra-high performance concrete in the marine environment. *Constr. Build. Mater.* **2021**, *291*, 123310. [[CrossRef](#)]
20. Lu, Z.; Feng, Z.; Yao, D.; Li, X.; Ji, H. Freeze-thaw resistance of Ultra-High performance concrete: Dependence on concrete composition. *Constr. Build. Mater.* **2021**, *293*, 123523. [[CrossRef](#)]
21. Dixit, A.; Verma, A.; Pang, S.D. Dual waste utilization in ultra-high performance concrete using biochar and marine clay. *Cem. Concr. Compos.* **2021**, *120*, 104049. [[CrossRef](#)]
22. Güneş, E.; Gesoğlu, M.; Mermerdaş, K. Improving strength, drying shrinkage, and pore structure of concrete using metakaolin. *Mater. Struct. Constr.* **2008**, *41*, 937–949. [[CrossRef](#)]
23. Siddique, R.; Klaus, J. Influence of metakaolin on the properties of mortar and concrete: A review. *Appl. Clay Sci.* **2009**, *43*, 392–400. [[CrossRef](#)]
24. Zhan, P.-M.; He, Z.-H.; Ma, Z.-M.; Liang, C.-F.; Zhang, X.-X.; Abreham, A.A.; Shi, J.-Y. Utilization of nano-metakaolin in concrete: A review. *J. Build. Eng.* **2020**, *30*, 101259. [[CrossRef](#)]
25. Raheem, A.A.; Abdulwahab, R.; Kareem, M.A. Incorporation of metakaolin and nanosilica in blended cement mortar and concrete—A review. *J. Clean. Prod.* **2021**, *290*, 125852. [[CrossRef](#)]
26. Sabir, B.; Wild, S.; Bai, J. Metakaolin and calcined clays as pozzolans for concrete: A review. *Cem. Concr. Compos.* **2001**, *23*, 441–454. [[CrossRef](#)]
27. Elahi, M.M.A.; Shearer, C.R.; Naser Rashid Reza, A.; Saha, A.K.; Khan, M.N.N.; Hossain, M.M.; Sarker, P.K. Improving the sulfate attack resistance of concrete by using supplementary cementitious materials (SCMs): A review. *Constr. Build. Mater.* **2021**, *281*, 122628. [[CrossRef](#)]
28. Panesar, D.K.; Zhang, R. Performance comparison of cement replacing materials in concrete: Limestone fillers and supplementary cementing materials—A review. *Constr. Build. Mater.* **2020**, *251*, 118866. [[CrossRef](#)]
29. Al Menhosh, A.; Wang, Y.; Wang, Y.; Augustus-Nelson, L. Long term durability properties of concrete modified with metakaolin and polymer admixture. *Constr. Build. Mater.* **2018**, *172*, 41–51. [[CrossRef](#)]
30. Hossain, M.M.; Karim, M.R.; Hasan, M.; Hossain, M.K.; Zain, M.F.M. Durability of mortar and concrete made up of pozzolans as a partial replacement of cement: A review. *Constr. Build. Mater.* **2016**, *116*, 128–140. [[CrossRef](#)]